



中国科学院高能物理研究所
Institute of High Energy Physics
Chinese Academy of Sciences



Run3 ECAL calibration and performance

Tianyu Cao

16th France-China Particle Physics Network/Laboratory workshop (FCPPN/L 2025)

21-25 July, 2025

Haitian Grand Theatre Hotel, Qingdao

FCPPN/L 2025



2025/7/21

- IP2I (former IPNL) contributed significantly to the construction of CMS ECAL subdetector
- Both IP2I and IHEP have been contributing significantly to the CMS ECAL performance studies
- One of IHEP members is currently one of the Level-2 conveners of the ECAL Detector Performance Group

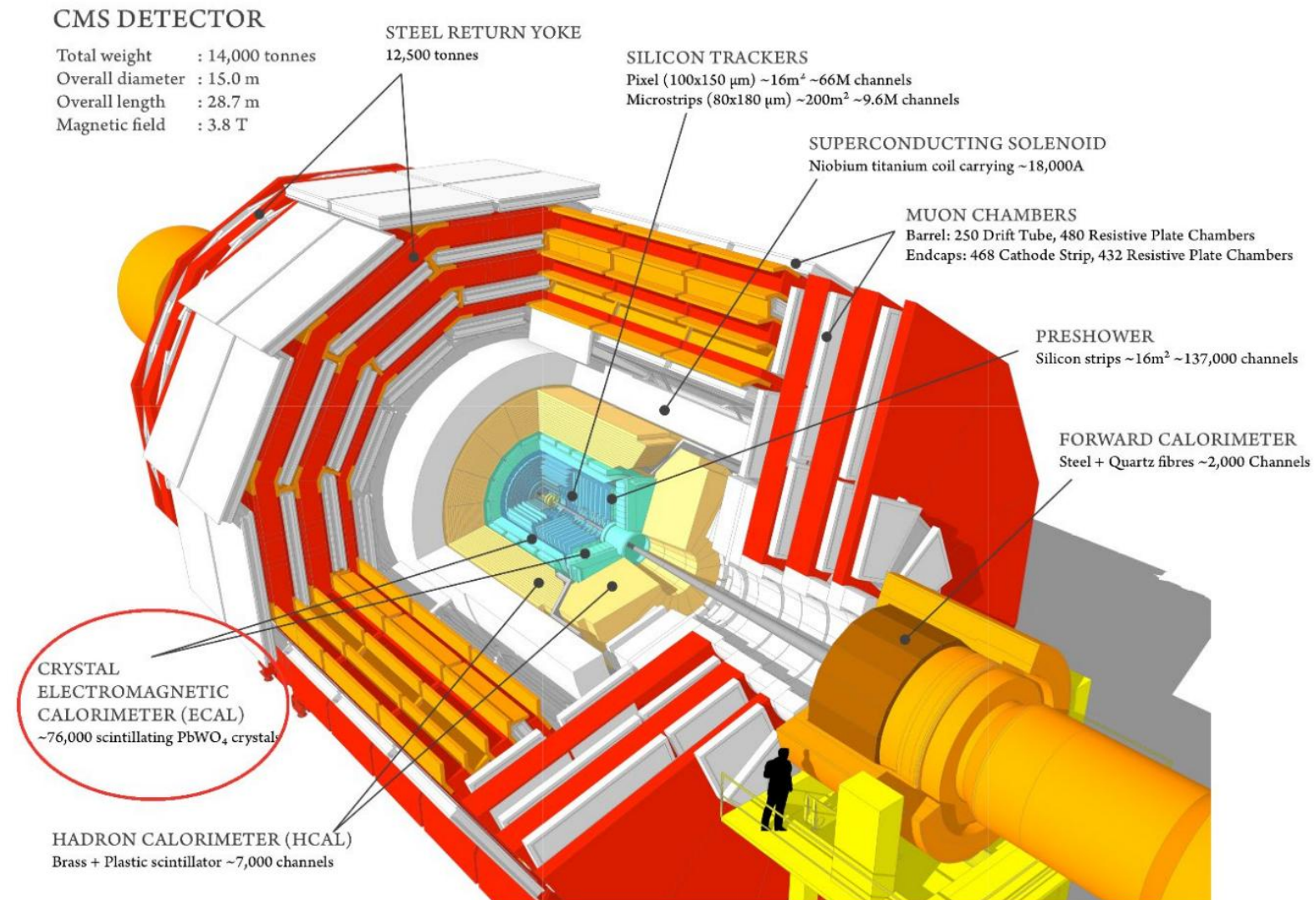


CMS Electromagnetic Calorimeter (ECAL)

CMS is a general-purpose detector designed to

- test Standard Model (SM) predictions
- search for new physics beyond the SM

The electromagnetic calorimeter plays a crucial role in many CMS physics analyses that involve electrons/photons/jets



Electromagnetic Calorimeter (ECAL)

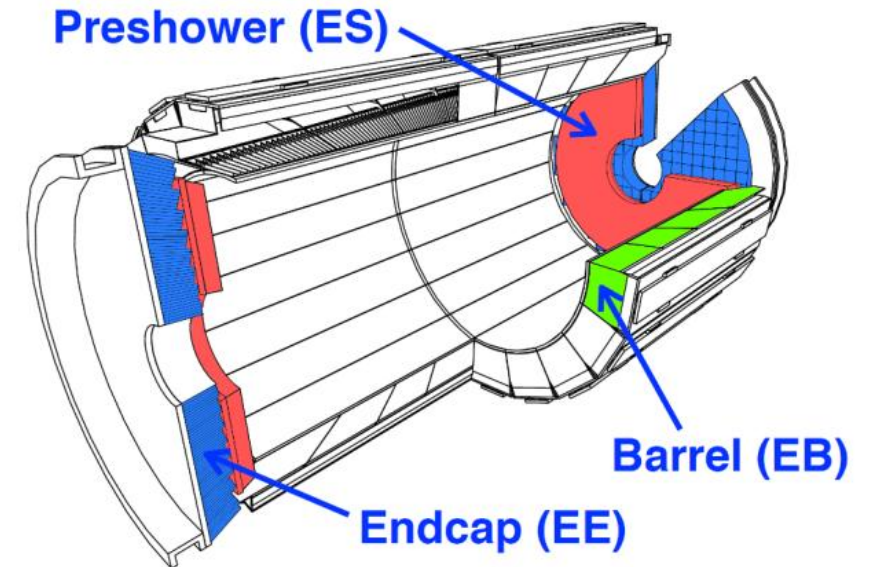
The Electromagnetic Calorimeter (ECAL) is a homogeneous calorimeter composed of 75,848 lead tungstate crystals PbWO_4

Coverage:

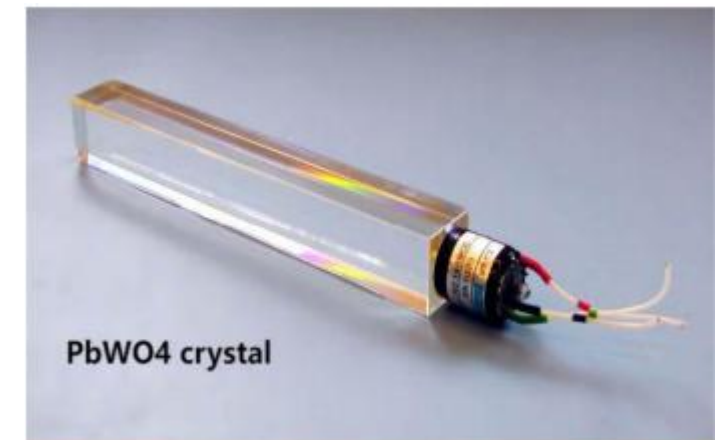
- ECAL Barrel (EB) : $|\eta| < 1.479$
- ECAL Endcap (EE): $1.479 < |\eta| < 3.0$
- ECAL Preshower (ES): $1.65 < |\eta| < 2.6$

ECAL provides efficient and accurate reconstruction of photons and electrons, which is crucial for many physics analyses:

- Studies of low energy multi lepton events
- Precise measurements of the Higgs boson
- Searches for high mass resonant particles at the TeV energy scale



ECAL



ECAL signal reconstruction

Electromagnetic particles deposit their energy over several ECAL crystals

- dynamic clustering algorithms used to collect the energy deposits in ECAL

The reconstructed energy of electrons and photons is estimated by:

$$E_{e,\gamma} = E_{e,\gamma} \times [G \times \sum_i (A_i \times LC_i \times IC_i) + E_{ES}]$$

$E_{e,\gamma}$: cluster correction obtained from a regression method

G : global scale factor for the analog-to-digital converter to actual energy value conversion

i : Each crystal in the cluster

A_i : the reconstructed signal amplitude

LC_i : laser correction: correct for crystal transparency loss

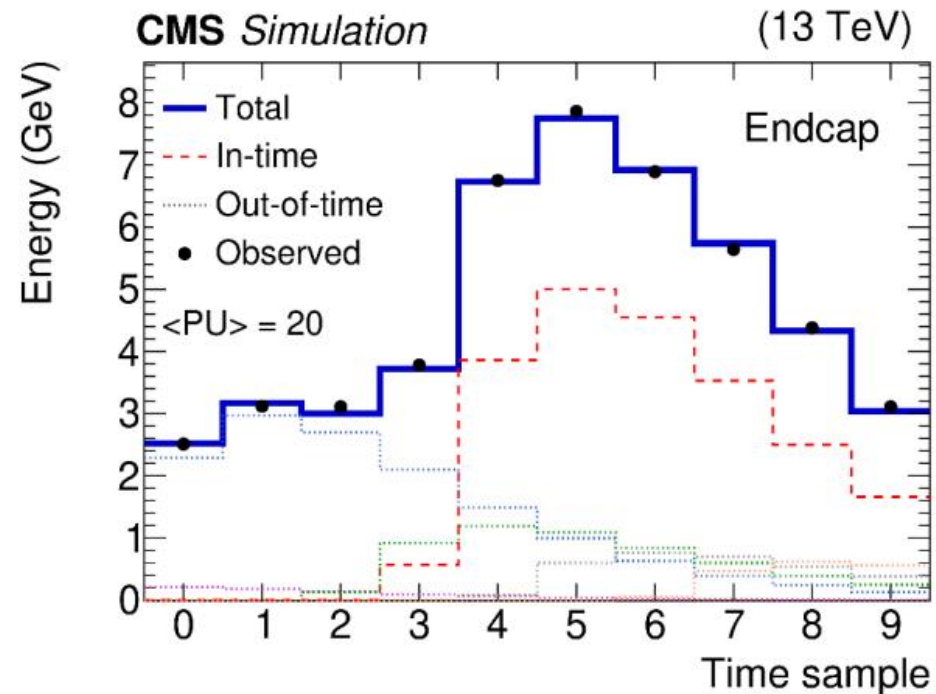
IC_i : intercalibration: equalize the channel response at same η

E_{ES} : preshower energy

ECAL signal reconstruction

Signal amplitude reconstruction (A_i):

- The multifit method: 10 digitized ECAL pulse samples recorded for signal amplitude reconstruction
- Fit one in-time pulse and up to 9 out-of-time (OOT) pulses
- The out-of-time pulses are obtained by shifting the in-time pulse in 25 ns steps

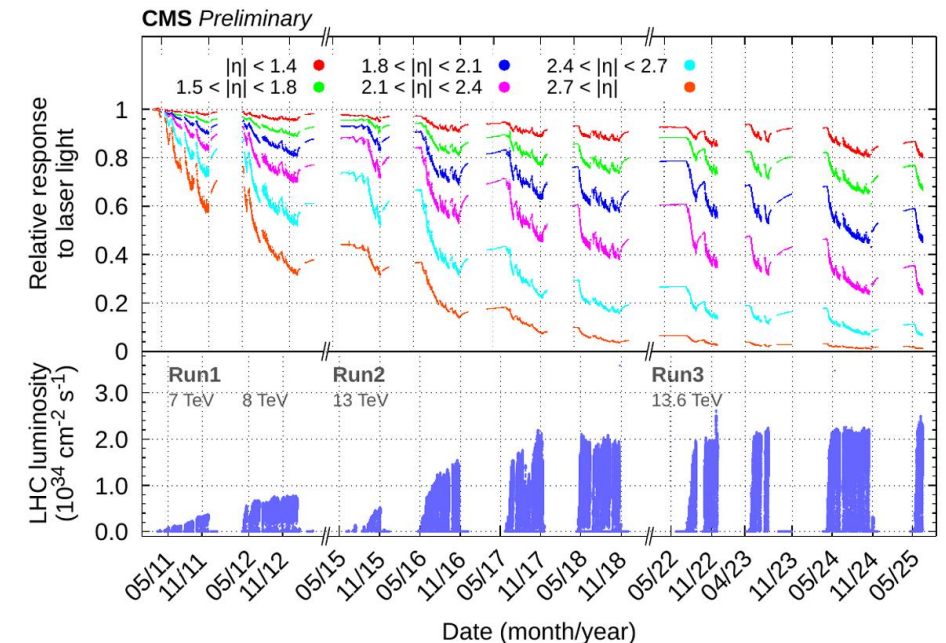
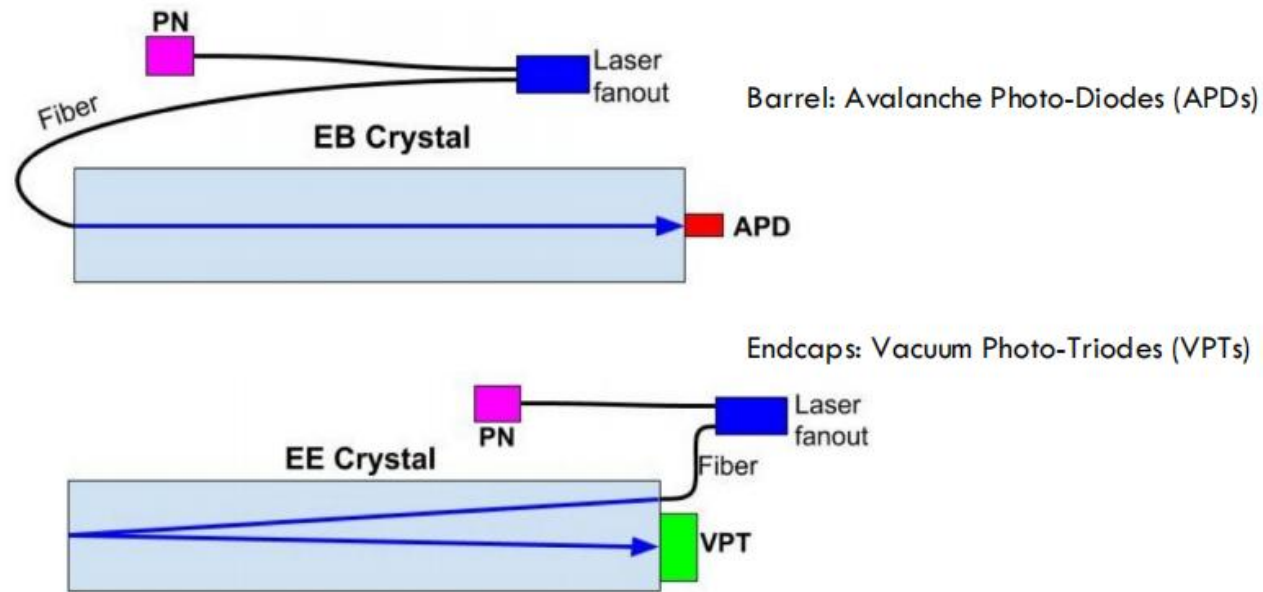


Pulses fitting

ECAL signal reconstruction

Laser Correction (LC_i):

- Due to ionizing radiation, the transparency of the PbWO_4 crystals in the ECAL gradually decreases over time
- A dedicated laser monitoring system is designed to provide corrections for transparency changes
 - injects laser light with a wavelength of 447nm into each crystal
 - relates ECAL channel response variation to changes in the scintillation signal
 - measures the calibration point per crystal every 40 minutes
 - obtains and applies corrections within 48 hours for the prompt reconstruction

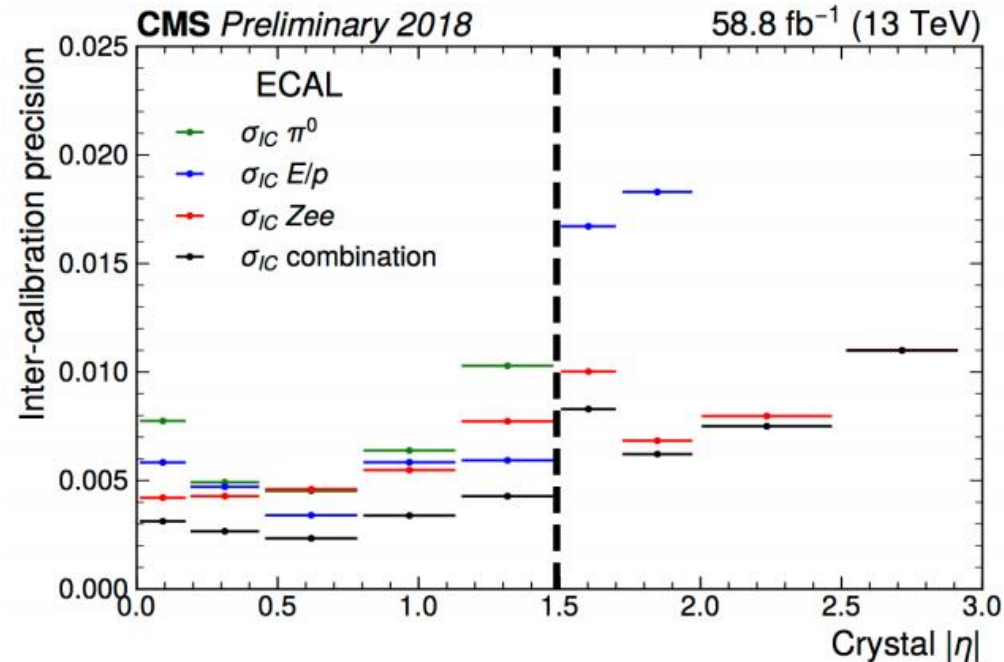
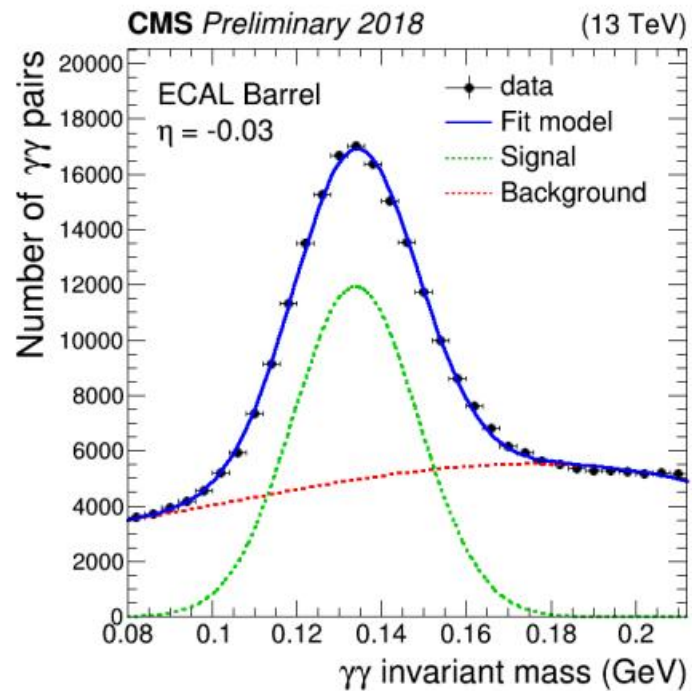


ECAL signal reconstruction

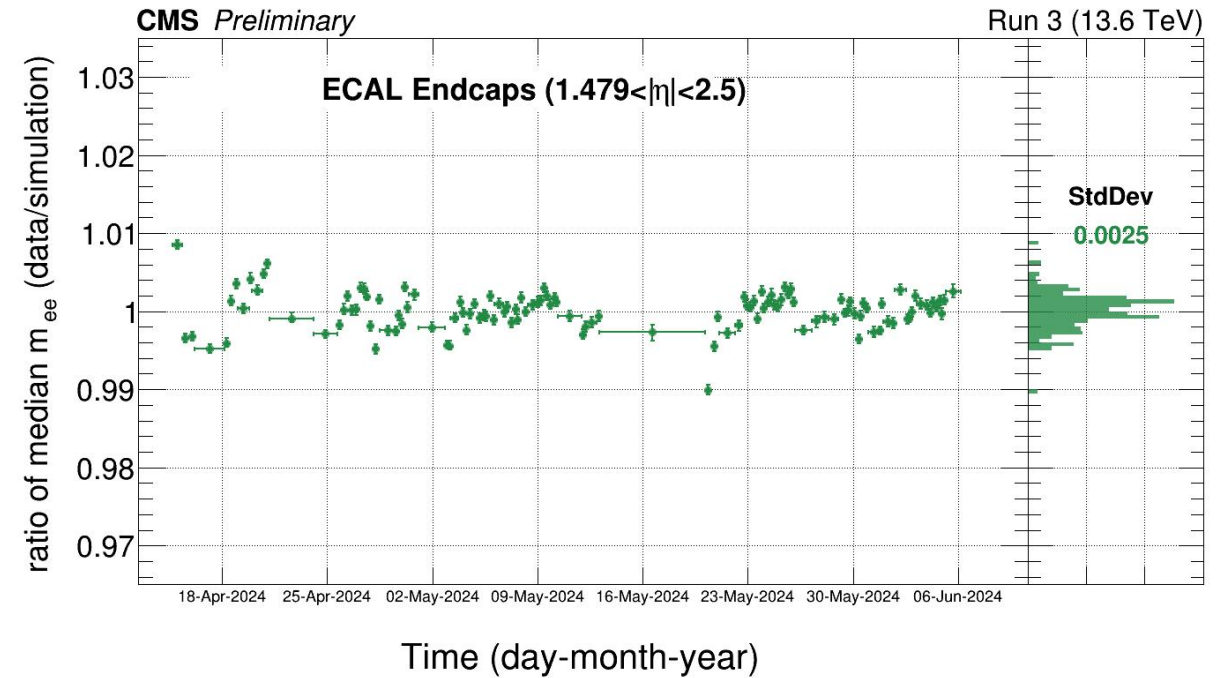
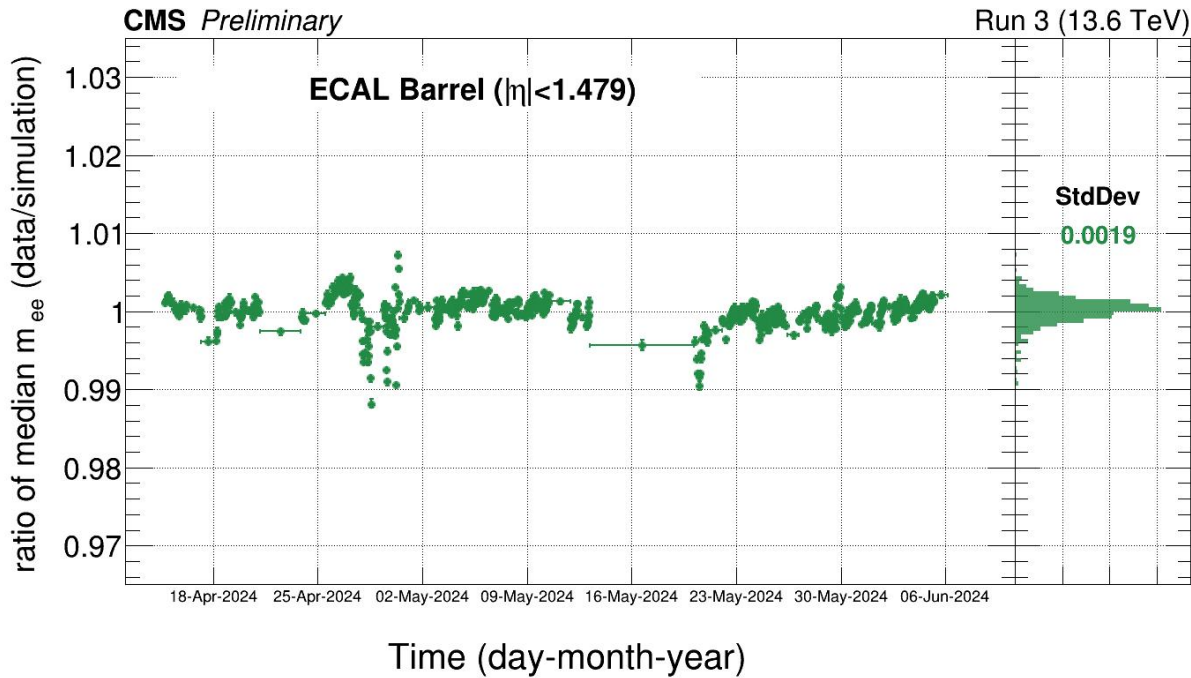
Intercalibration (IC_i) : equalize the ECAL response for different crystals at the same η coordinate

A combination of several methods based on different physics signals

- π^0 mass: exploit reconstructed π^0 mass with its decay of photon pairs
- E/p: comparison of the ECAL energy to the tracker momentum for isolated electrons from W/Z boson decay
- Zee: exploit the invariant mass reconstructed with electron pairs from Z decays



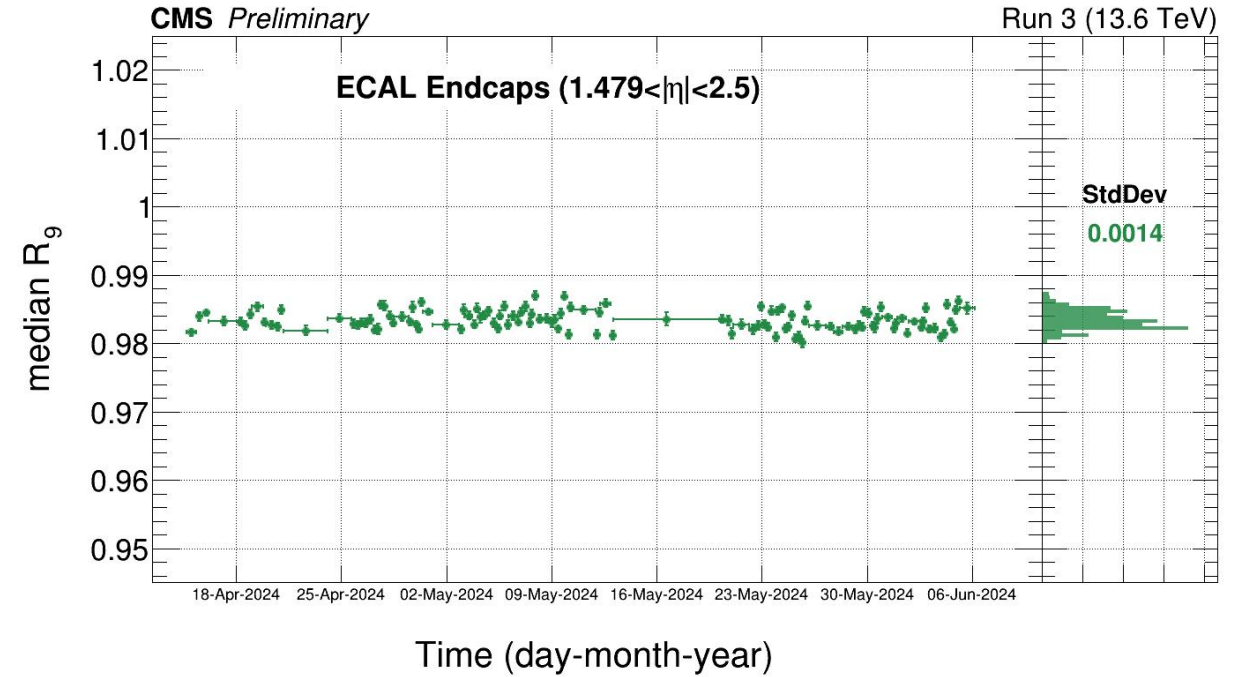
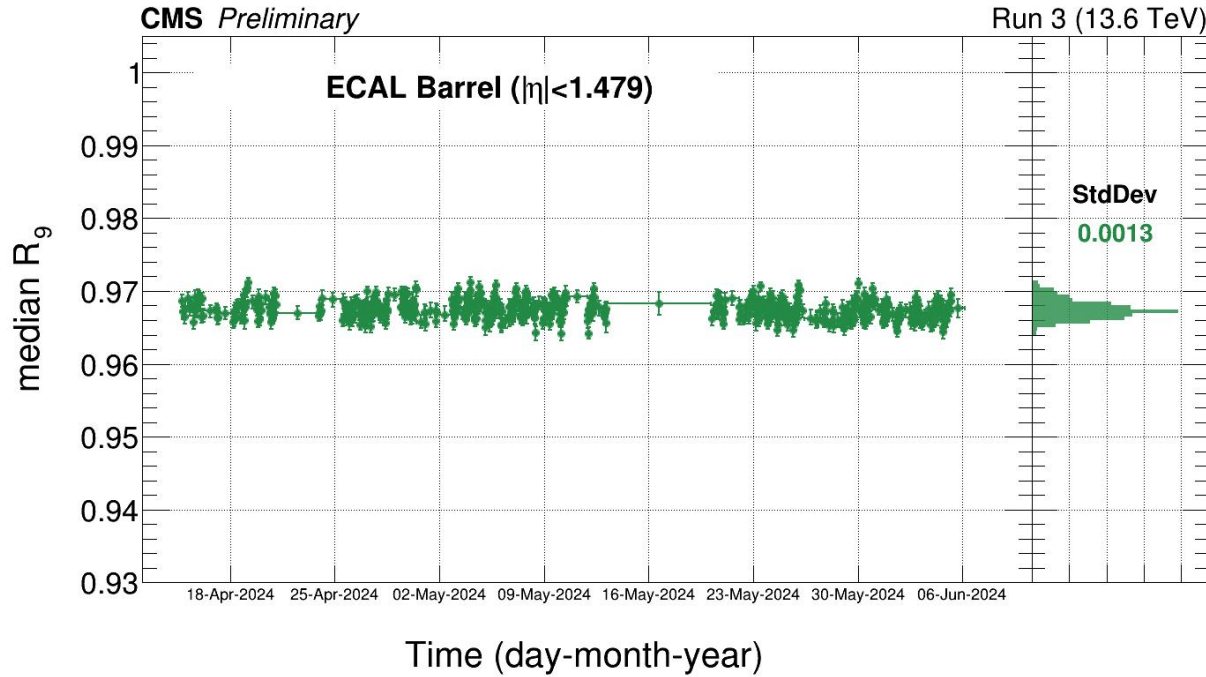
ECAL stability - di-electron mass over time (scaled by simulation)



Time stability of the di-electron invariant mass comparing between data and simulation for the early 2024 data-taking period using $Z \rightarrow ee$.

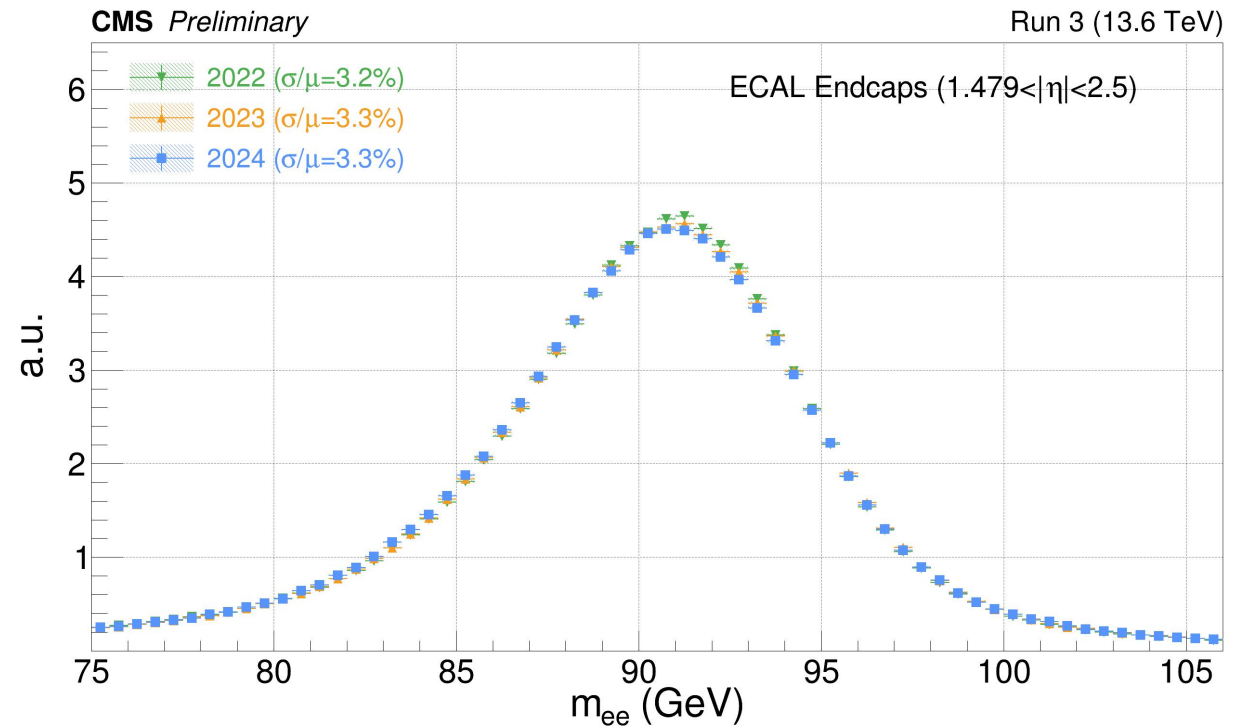
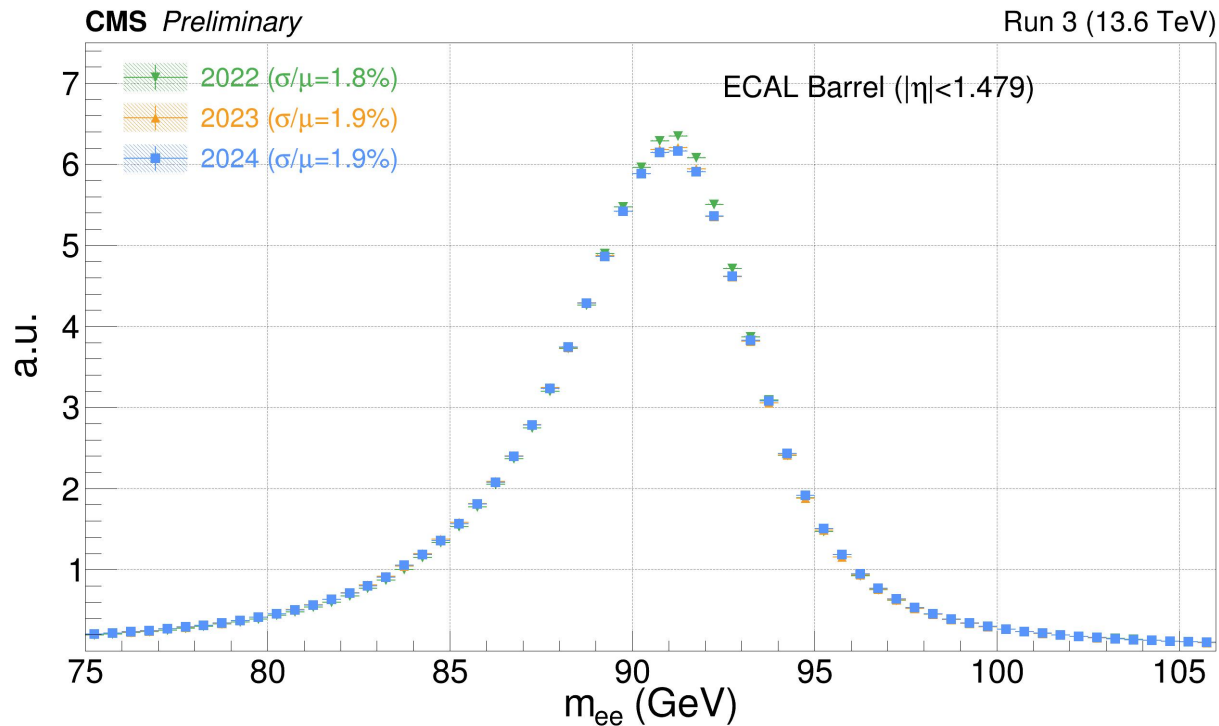
The plot shows the time stability of the di-electron invariant mass median ratio of data and simulation with a refined re-calibration for dataset from early 2024. Both electrons are required to be in the ECAL Barrel or in the ECAL Endcaps. The di-electron invariant mass is required to be between 70 GeV and 110 GeV. Each time bin has around 10000 events. The error bar on the points denotes the statistical uncertainty (at 68% confidence level) on the median. The right panel shows the distribution of the median ratios.

R9 stability



Stability of the shower shape of the electromagnetic deposit in the ECAL for the leading electron from Z decays. The plot shows the time stability of the shower shape of the leading electron in Z decays with a refined re-calibration for dataset from early 2024. The event selection requires two electrons to be in the ECAL Barrel or in the ECAL Endcaps. The di-electron invariant mass is required to be between 70 GeV and 110 GeV. Each time bin has around 10000 events. The error bar on the points denotes the statistical uncertainty (at 68% confidence level) on the median. The right panel shows the distribution of the medians. The shower shape is measured by the variable R9, defined as in [EGM-18-002](#), the ratio of the energy deposit in the 3x3 crystal matrix around the seed crystal to that in the supercluster. The shower shapes of the electromagnetic deposit in the ECAL are very stable in 2024.

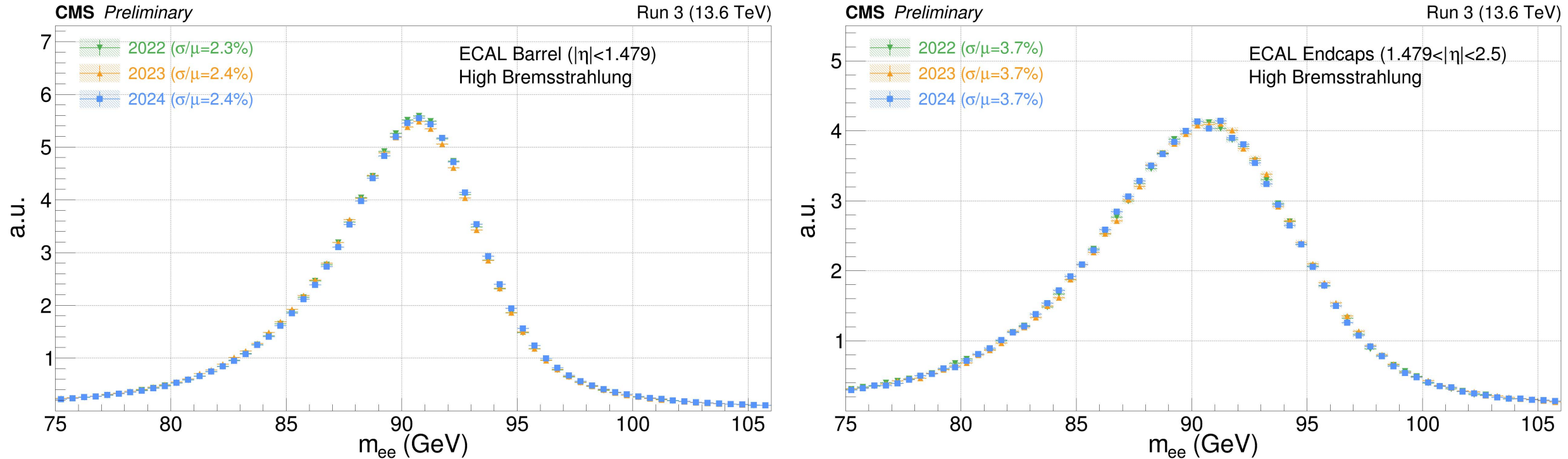
Di-electron mass inclusive



Invariant mass distribution for electron pairs from Z boson decays.

The plot shows the invariant mass distribution comparing 2022, 2023 and early 2024 dataset using $Z \rightarrow ee$ events with a refined re-calibration. The event selection requires two electrons to be in the ECAL Barrel or in the ECAL Endcaps. For candidates in the Endcaps, the electron pseudorapidity is required to be lower than 2.5. Here, σ represents the Gaussian width, reflecting the detector resolution, and μ represents the fitted Z peak mean.

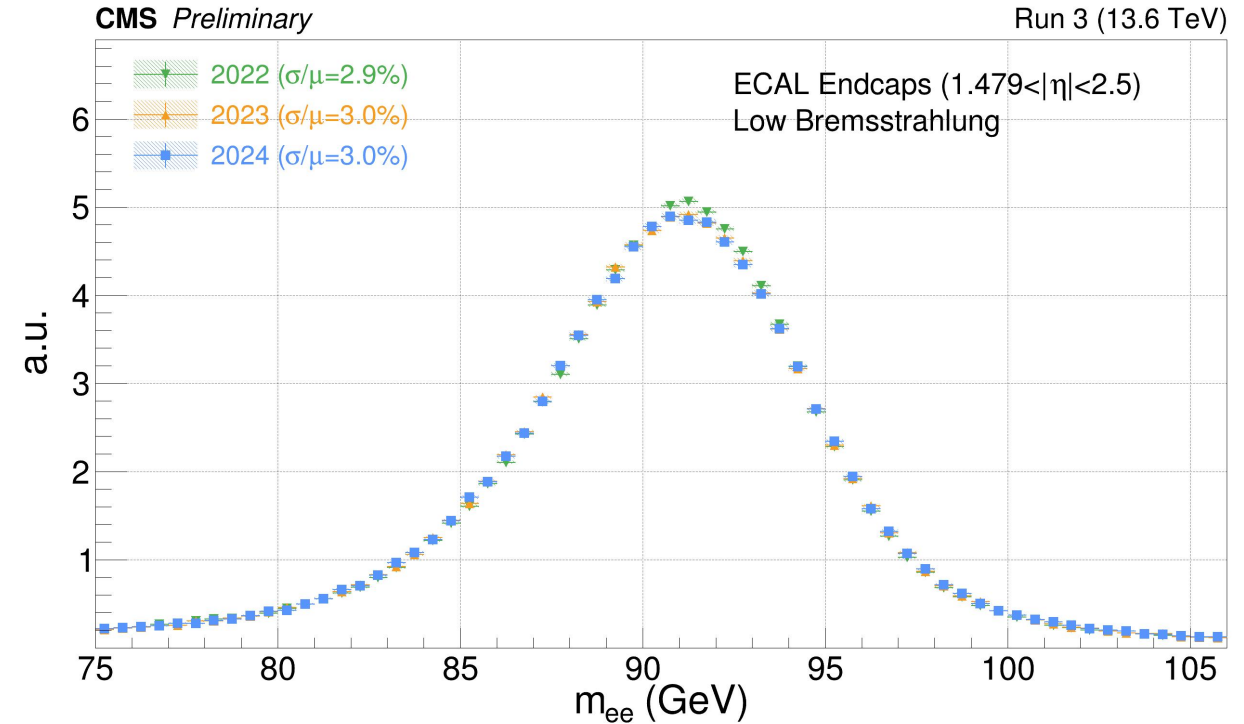
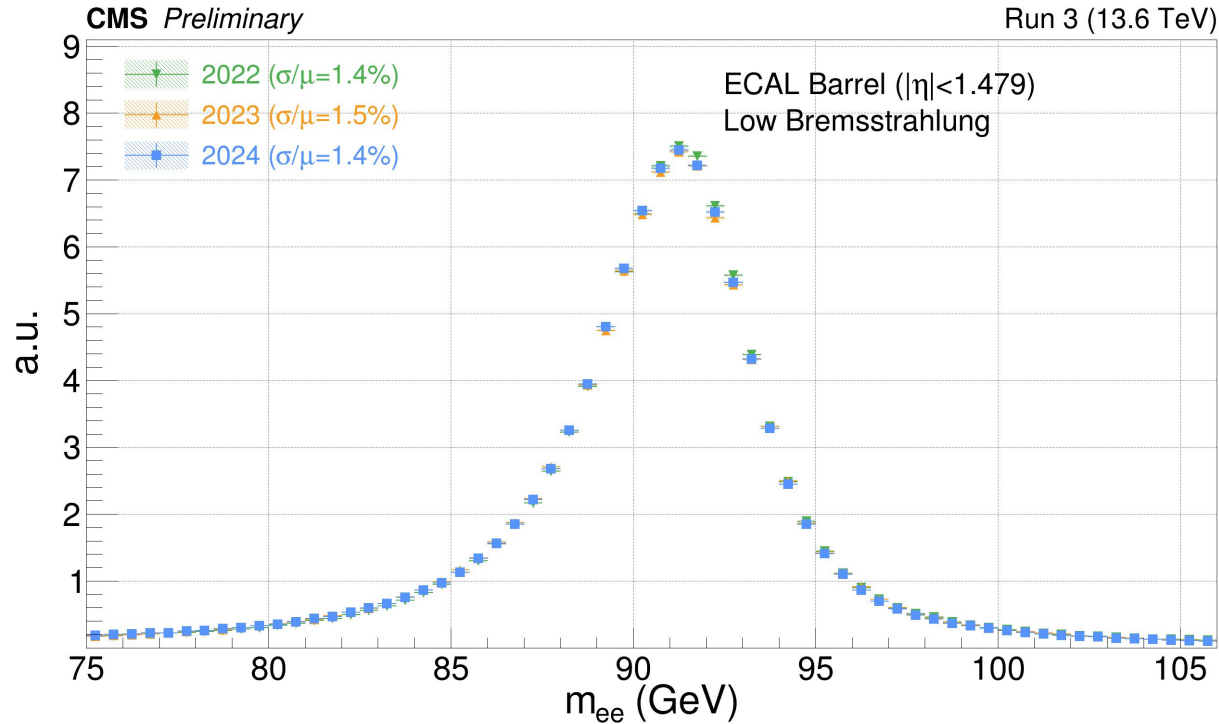
Di-electron mass high bremsstrahlung



Invariant mass distribution for electron pairs from Z boson decays using high-bremsstrahlung electrons.

The plot shows the invariant mass distribution comparing 2022, 2023 and early 2024 dataset using $Z \rightarrow ee$ events with a refined re-calibration. The event selection requires two electrons to be in the ECAL Barrel or in the ECAL Endcaps. For candidates in the Endcaps, the electron pseudorapidity is required to be lower than 2.5. Here, σ represents the Gaussian width, reflecting the detector resolution, and μ represents the fitted Z peak mean. For high-bremsstrahlung electrons, the shower shape variable of R9, defined as in [EGM-18-002](#), is required to be greater than 0.975.

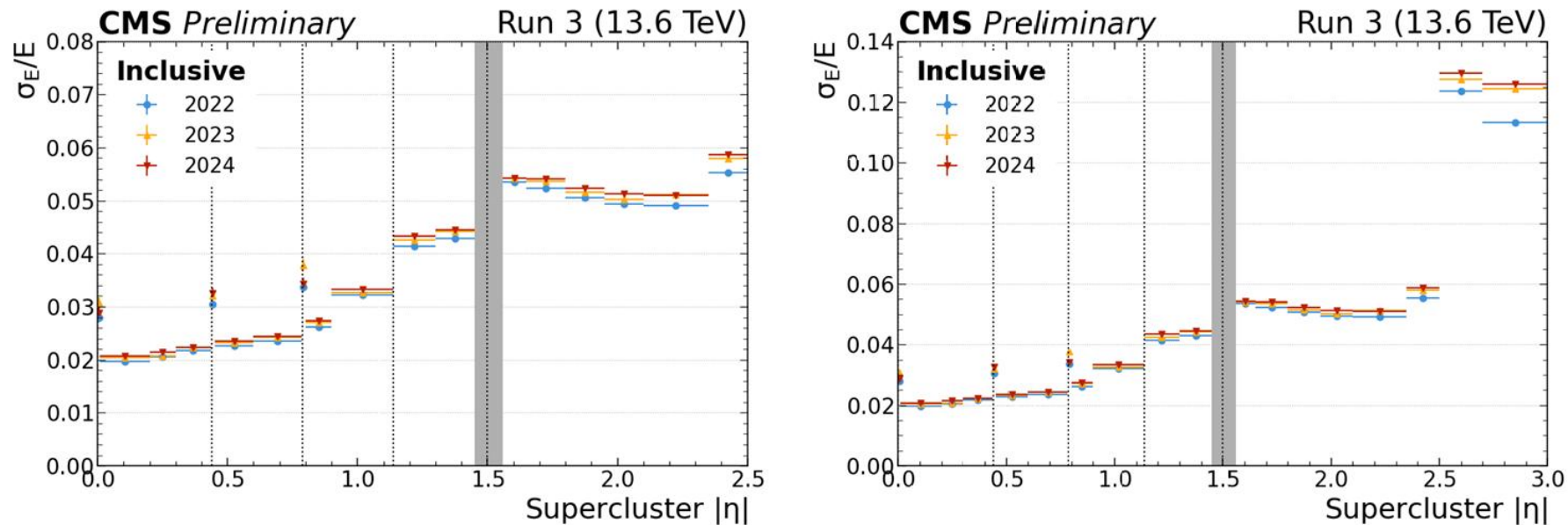
Di-electron mass low bremsstrahlung



Invariant mass distribution for electron pairs from Z boson decays using low-bremsstrahlung electrons.

The plot shows the invariant mass distribution comparing 2022, 2023 and early 2024 dataset using $Z \rightarrow ee$ events with a refined re-calibration. The event selection requires two electrons to be in the ECAL Barrel or in the ECAL Endcaps. For candidates in the Endcaps, the electron pseudorapidity is required to be lower than 2.5. Here, σ represents the Gaussian width, reflecting the detector resolution, and μ represents the fitted Z peak mean. For low-bremsstrahlung electrons, the shower shape variable of R9, defined as in [EGM-18-002](#), is required to be less than 0.975.

ECAL Resolution – inclusive



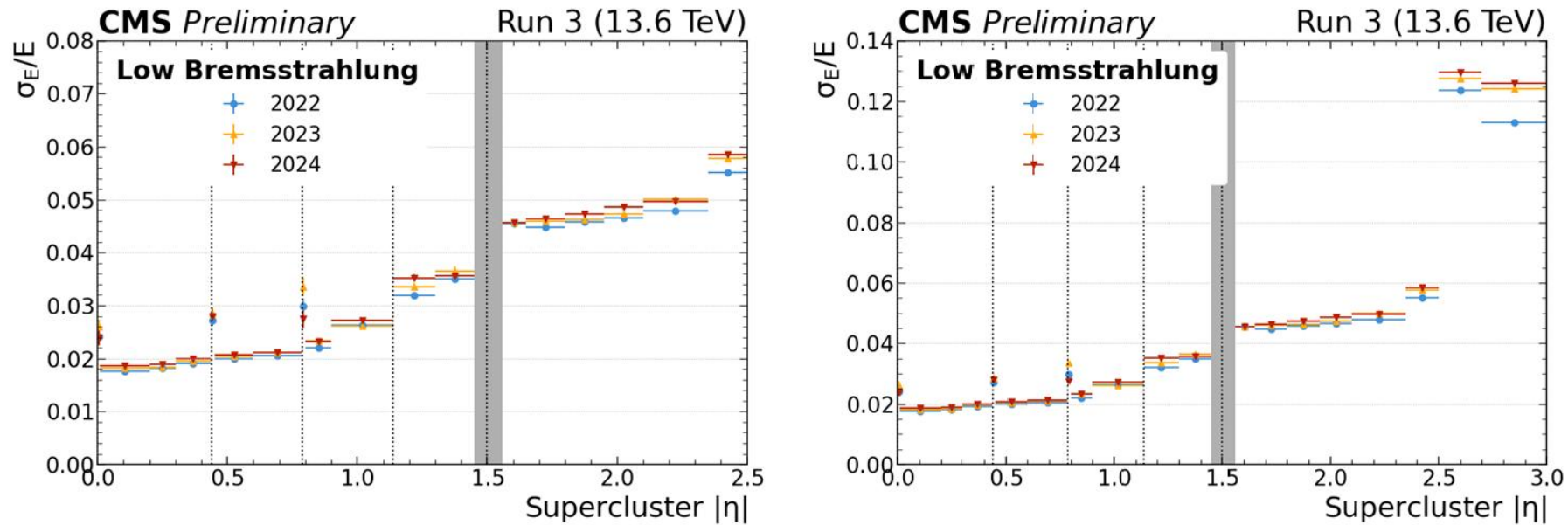
ECAL energy resolution for electrons measured on $Z \rightarrow ee$ events unfolded in bins of pseudorapidity η . The resolution is shown separately for all electrons ("inclusive").

The plots compare the resolution achieved after a refined calibration of the data collected during 2022, 2023 and the initial part of 2024 at 13.6 TeV. The vertical dotted lines mark the boundaries between the ECAL modules in the barrel, where a slight worsening of the resolution is observed due to the material of the mechanical structures. The shaded grey band corresponds to the ECAL Barrel / ECAL Endcap transition.

The left plots show the resolution within the pseudorapidity region of the CMS tracker, whereas the right plots cover the whole ECAL pseudorapidity range.

A stable ECAL energy resolution is observed between 2022, 2023 and the initial part of 2024 despite the increased LHC instantaneous luminosity and the ageing of the detector.

ECAL Resolution – low bremsstrahlung



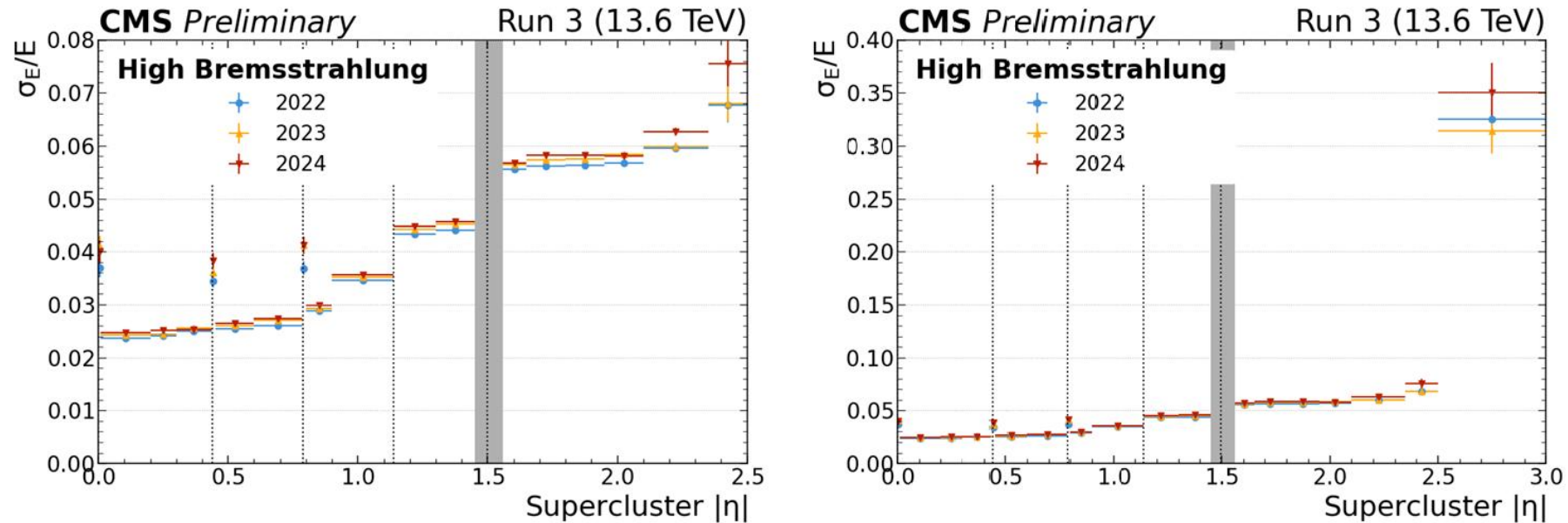
ECAL energy resolution for electrons measured on $Z \rightarrow ee$ events unfolded in bins of pseudorapidity η . The resolution is shown separately for low-bremsstrahlung electrons.

The plots compare the resolution achieved after a refined calibration of the data collected during 2022, 2023 and the initial part of 2024 at 13.6 TeV. The vertical dotted lines mark the boundaries between the ECAL modules in the barrel, where a slight worsening of the resolution is observed due to the material of the mechanical structures. The shaded grey band corresponds to the ECAL Barrel / ECAL Endcap transition.

The left plots show the resolution within the pseudorapidity region of the CMS tracker, whereas the right plots cover the whole ECAL pseudorapidity range.

A stable ECAL energy resolution is observed between 2022, 2023 and the initial part of 2024 despite the increased LHC instantaneous luminosity and the ageing of the detector.

ECAL Resolution – high bremsstrahlung



ECAL energy resolution for electrons measured on $Z \rightarrow ee$ events unfolded in bins of pseudorapidity η . The resolution is shown separately for high-bremsstrahlung electrons.

The plots compare the resolution achieved after a refined calibration of the data collected during 2022, 2023 and the initial part of 2024 at 13.6 TeV. The vertical dotted lines mark the boundaries between the ECAL modules in the barrel, where a slight worsening of the resolution is observed due to the material of the mechanical structures. The shaded grey band corresponds to the ECAL Barrel / ECAL Endcap transition.

The left plots show the resolution within the pseudorapidity region of the CMS tracker, whereas the right plots cover the whole ECAL pseudorapidity range.

A stable ECAL energy resolution is observed between 2022, 2023 and the initial part of 2024 despite the increased LHC instantaneous luminosity and the ageing of the detector.

Calibration and optimization has been exploited in CMS ECAL

- challenging due to increased instantaneous luminosity and detector aging
- new multifit method for amplitude reconstruction
- frequent laser correction to stable ECAL response over time
- combined intercalibration to stable crystal response at same η

Outstanding performance of the CMS ECAL with calibration

- stable ECAL response over time with spread at $\sim 1\%$ level
- resolution of electrons between 2% and 5%
- ECAL performance stable over time despite much harsher environment and detector aging

Thanks!

Backup